


Orbital Angular Momentum Coupling in Elastic Photon-Photon ScatteringR. Aboushelbaya^{1,*}, K. Glize,² A. F. Savin,¹ M. Mayr,¹ B. Spiers,¹ R. Wang,¹ J. Collier,²
M. Marklund,³ R. M. G. M. Trines,² R. Bingham,^{2,4} and P. A. Norreys^{2,1,†}¹Clarendon Laboratory, University of Oxford, Parks Road, Oxford OX1 3PU, United Kingdom²Central Laser Facility, STFC Rutherford Appleton Laboratory, Didcot OX11 0QX, United Kingdom³Department of Physics, University of Gothenburg, SE-41296 Gothenburg, Sweden⁴Department of Physics, University of Strathclyde, Strathclyde G4 0NG, United Kingdom (Received 18 February 2019; revised manuscript received 20 May 2019; published 13 September 2019)

In this Letter, we investigate the effect of orbital angular momentum (OAM) on elastic photon-photon scattering in a vacuum for the first time. We define exact solutions to the vacuum electromagnetic wave equation which carry OAM. Using those, the expected coupling between three initial waves is derived in the framework of an effective field theory based on the Euler-Heisenberg Lagrangian and shows that OAM adds a signature to the generated photons thereby greatly improving the signal-to-noise ratio. This forms the basis for a proposed high-power laser experiment utilizing quantum optics techniques to filter the generated photons based on their OAM state.

DOI: [10.1103/PhysRevLett.123.113604](https://doi.org/10.1103/PhysRevLett.123.113604)

Photon-photon scattering in vacuum is an effect that has attracted considerable interest over the past few decades [1,2]. In classical electromagnetism, the linearity of Maxwell's equations indicates that scattering between photons cannot happen in the vacuum. Nevertheless, results from quantum electrodynamics (QED) have shown that the vacuum is, in fact, nonlinear. This means that the aforementioned scattering is actually possible, albeit very difficult to observe [3]. Many different proposals have been made to detect such processes using microwave cavities [1], plasma channels [4], and high-power lasers [5,6]. The main obstacle to these schemes has been the relatively weak predicted signal compared to the noise inherent to any experiment. As such, scattering between real photons has yet to be observed in the vacuum.

In this Letter, we investigate the effect of orbital angular momentum (OAM) coupling in elastic photon-photon scattering, and we show, for the first time, that OAM contributes an additional unique signature that will help filter the background noise and, thus, is predicted to make the detection of these weak signals easier. OAM is a relatively recently understood degree of freedom of light that is distinct from the more widely understood spin angular momentum which is related to light's polarization [7]. It appears in electromagnetic modes which have an azimuthal phase dependence, $E(\mathbf{r}) \propto e^{i\ell\phi}$, where

conventionally ℓ denotes the OAM state of the mode. It should be noted that, here, ℓ represents the projection of OAM on the direction of propagation in contrast to its use in the quantum mechanical treatment of bound electronic states where it represents the absolute value of the "total" OAM. Interest in researching these modes has grown ever since they were shown to carry a quantized net angular momentum separate from their spin [8]. Since it is unbounded and can have any integer value, OAM has many potential applications in different fields including: enhanced imaging techniques, light manipulation, and high density coding of information for communication [7,9,10]. Consequentially, over the course of the previous two decades, the techniques required to efficiently generate OAM states, and detect and filter photons according to their OAM state (right down to the single-photon level) have been honed to a great level of precision [11,12]. For this reason, we are interested in investigating its impact on photon-photon scattering.

This Letter will be organized as follows: first, exact solutions to the electromagnetic wave equation which carry OAM will be discussed. These modes will then be used to investigate the effect of OAM on photon-photon interaction within the framework of an effective field theory [13]. Finally, a proposed experimental configuration will be presented that is expected to validate the accompanying theoretical work.

The simplest solution to the linear electromagnetic wave equation is the plane wave decomposition, where a plane wave is described by

$$\mathbf{E}(\mathbf{r}, t) = \mathcal{E}_0 e^{i(\mathbf{k}\cdot\mathbf{r} - \omega t)} \hat{\mathbf{n}}, \quad (1)$$

where \mathbf{k} is the wave vector, ω is the angular frequency, and $\hat{\mathbf{n}}$ is the polarization unit vector of the plane wave which

Published by the American Physical Society under the terms of the [Creative Commons Attribution 4.0 International license](https://creativecommons.org/licenses/by/4.0/). Further distribution of this work must maintain attribution to the author(s) and the published article's title, journal citation, and DOI.

necessarily satisfies the transversality condition ($\mathbf{k} \cdot \hat{\mathbf{n}} = 0$) arising from Maxwell's equations. Then, we consider an infinite superposition of plane waves whose wave vectors lie on the surface of a cone with half-angle α around the z axis

$$\mathbf{E}_l(\mathbf{r}, t) = \frac{\mathcal{E}_0}{2\pi} \int_0^{2\pi} (i)^l e^{i[\mathbf{k}(\phi_k) \cdot \mathbf{r} - \omega_0 t + l\phi_k]} \hat{\mathbf{n}}(\phi_k) d\phi_k, \quad (2)$$

$$\mathbf{k}(\phi_k) = k \cos(\alpha) \hat{\mathbf{z}} - k \sin(\alpha) [\cos(\phi_k) \hat{\mathbf{x}} + \sin(\phi_k) \hat{\mathbf{y}}], \quad (3)$$

$$\hat{\mathbf{n}}(\phi_k) = \sin(\phi_k) \hat{\mathbf{x}} - \cos(\phi_k) \hat{\mathbf{y}}, \quad (4)$$

where $l \in \mathbb{Z}$ is the azimuthal mode number. \mathbf{E}_l , then, is obviously an exact solution to the electromagnetic wave equation as it is a linear superposition of exact solutions. Its integral representation can be simplified by decomposing the trigonometric functions into their exponential form and using the fact that $(1/2\pi) \int_0^{2\pi} e^{i[l\phi - x \sin(\phi)]} d\phi = J_l(x)$ [14], where $J_l(x)$ is the l th order Bessel function of the first kind. Thus, the electric field in Eq. (2) can be rewritten in cylindrical coordinates (z, ρ, ϕ) as

$$\mathbf{E}_l(z, \rho, \phi, t) = \mathcal{E}_0 e^{i(\kappa z - \omega t + l\phi)} \left(-\frac{l J_l(\beta\rho)}{\beta\rho} \hat{\mathbf{e}}_\rho + i \frac{J_{l+1}(\beta\rho) - J_{l-1}(\beta\rho)}{2} \hat{\mathbf{e}}_\phi \right), \quad (5)$$

where $\kappa = k \cos(\alpha)$ and $\beta = k \sin(\alpha)$. The corresponding magnetic field can then be calculated from Eq. (5) using Maxwell's equations ($\nabla \times \mathbf{E}_l = -\partial \mathbf{B}_l / \partial t$). This solution can be seen as an OAM-carrying extension of the electromagnetic Bessel modes. One of the interesting properties of Bessel modes is that they propagate without diffraction as can be seen by noting that the radial profile of the field is independent of the longitudinal position along the direction of propagation. True Bessel beams are unphysical, as they carry infinite energy. However, Bessel-like modes, which retain some of the aforementioned interesting properties over a known coherence length, have been generated using axicon lenses [15]. When considering the case of $l \neq 0$, the field has an azimuthal phase dependence, and therefore, as shown in [8], it carries nonzero OAM. This can be confirmed by calculating the time-averaged angular momentum density of the field $\langle \mathfrak{L} \rangle = (1/2) \mathbf{r} \times \Re(\mathbf{E}^* \times \mathbf{B})$.

$$\langle \mathfrak{L} \rangle = \frac{\epsilon_0 \mathcal{E}_0^2}{c} \left(\frac{l}{k_0} J_l^2(\beta\rho) \hat{\mathbf{z}} - \frac{l z \sin(\alpha)}{\beta\rho} J_l^2(\beta\rho) \hat{\rho} - \rho \cos(\alpha) \frac{J_{l+1}^2(\beta\rho) - J_{l-1}^2(\beta\rho)}{2} \hat{\phi} \right). \quad (6)$$

If $\langle \mathfrak{L} \rangle$ is integrated over a finite circular transverse profile of the field, only the z component of the angular momentum density contributes as the polar unit vectors integrate to 0. This results in a total angular momentum $\langle \mathbf{L} \rangle \propto l \hat{\mathbf{z}}$.

It should be noted that this method of defining light modes that carry OAM differs from the standard approach of considering Laguerre-Gaussian (LG) modes [8]. The method used here offers two advantages, the first being that the field defined in Eq. (5) is, by construction, divergence-free and, hence, an exact solution of Maxwell's equations. Second, it offers a simple representation of OAM beams as a superposition of plane waves which proves highly advantageous when calculating the nonlinear interaction terms compared to the LG modes which contain a complicated envelope that makes the calculation intractable.

Classically, photon-photon scattering is physically impossible since Maxwell's equations are linear [16], meaning that any superposition of solutions to the wave equation is, itself, a solution. However, the full quantum electrodynamic treatment of the vacuum field predicts the existence of vacuum polarization and the possibility of photon-photon scattering mediated by virtual electron-positron pairs [3]. The exact treatment of this problem is quite challenging; however, the interaction can be approximated by the Euler-Heisenberg Lagrangian which accounts for this vacuum polarization up to one loop in the corresponding Feynman diagram, thereby accounting for the lowest order contribution to the photon-photon QED scattering amplitude. It can be written in Gaussian units, in the limit for fields oscillating slower than the Compton frequency, as [13]

$$\mathcal{L} = \frac{1}{8\pi} ((\mathbf{E}^2 - \mathbf{B}^2) + \xi[(\mathbf{E}^2 - \mathbf{B}^2)^2 + 7(\mathbf{E} \cdot \mathbf{B})^2]), \quad (7)$$

where $\xi = [(\hbar e^4)/(45\pi^2 m^4 c^7)]$. A modified electromagnetic wave equation can then be derived using the Euler-Lagrangian equations. The quartic corrections to the Lagrangian lead to a nonlinear source term for the wave equation, even in the vacuum.

$$\partial^\mu \partial_\mu \mathbf{E} = 4\pi [c^2 \nabla(\nabla \cdot \mathbf{P}) - \partial_t(\partial_t \mathbf{P} + c \nabla \times \mathbf{M})], \quad (8)$$

where $\partial^\mu \partial_\mu = \partial_t^2 - c^2 \nabla^2$, and \mathbf{M} and \mathbf{P} are the effective vacuum magnetization and polarization, respectively, described by

$$\mathbf{M} = (4\pi)^{-1} \xi [-2(\mathbf{E}^2 - \mathbf{B}^2) \mathbf{B} + 7(\mathbf{E} \cdot \mathbf{B}) \mathbf{E}], \quad (9)$$

$$\mathbf{P} = (4\pi)^{-1} \xi [2(\mathbf{E}^2 - \mathbf{B}^2) \mathbf{E} + 7(\mathbf{E} \cdot \mathbf{B}) \mathbf{B}]. \quad (10)$$

These equations indicate that the source term in Eq. (8) has a nonlinear cubic dependence on the electromagnetic fields. Therefore, if we start with three plane waves $(\mathbf{k}_i, \omega_i)_{i \in \{1,2,3\}}$, it is clear that the three modes will mix generating a fourth wave (\mathbf{k}_4, ω_4) that satisfies the following energy and momentum matching conditions

$$\mathbf{k}_1 + \mathbf{k}_2 = \mathbf{k}_3 + \mathbf{k}_4, \quad \omega_1 + \omega_2 = \omega_3 + \omega_4. \quad (11)$$

There are, of course, many other interaction terms that involve different combinations of the three initial waves. However, in the rest of this Letter, only terms that correspond to the matching conditions in Eq. (11) will be considered. This is because it is the most convenient generated wave to measure experimentally and allows for flexibility in the geometrical setup of the incoming beams as will be seen in the following parts. This does not necessarily mean that the other interaction terms are particularly weaker. However, they are also not any stronger, and waves generated through them will have frequencies and directions of propagation (and different OAM states as will be seen later on) different from Eq. (11), meaning that they can safely be neglected when estimating the number of detected photons in the experimental geometry that will be considered later on.

Let the three initial plane waves be $\mathbf{E}_1 = E_1 e^{i(k_0 x - \omega_0 t)} \hat{\mathbf{y}}$, $\mathbf{E}_2 = E_2 e^{i(-k_0 x - \omega_0 t)} \hat{\mathbf{z}}$, and $\mathbf{E}_3 = (i)^l E_3 e^{i[\mathbf{k}_3(\phi_k) \cdot \mathbf{r} - \omega_0 t]} e^{il\phi_k} \hat{\mathbf{n}}(\phi_k)$ where $\mathbf{k}_3(\phi_k) = k_0 \cos(\alpha) \hat{\mathbf{z}} - k_0 \sin(\alpha) [\cos(\phi_k) \hat{\mathbf{x}} + \sin(\phi_k) \hat{\mathbf{y}}]$ and $\hat{\mathbf{n}}(\phi_k) = \sin(\phi_k) \hat{\mathbf{x}} - \cos(\phi_k) \hat{\mathbf{y}}$. It is clear that \mathbf{E}_3 is a plane wave that lies on the surface of a cone with half-angle α similar to the aforementioned case. Further, α is considered to be very small, which is a reasonable assumption with Bessel beams, as they are generally generated with axicon lenses which have a very shallow angle. Keeping only the interaction terms of Eq. (8) that are resonant for the generated fourth wave \mathbf{E}_4 . The nonlinear wave equation can then be written as [17]

$$\partial^\mu \partial_\mu \mathbf{E}_4 \approx (-i)^l \omega_0^2 \xi \hat{\mathbf{v}}(\phi_k) E_1 E_2 E_3^* e^{i[\mathbf{k}_4(\phi_k) \cdot \mathbf{r} - \omega_0 t - l\phi_k]}, \quad (12)$$

where $\hat{\mathbf{v}}(\phi_k) = \cos(\alpha) \cos(\phi_k) \hat{\mathbf{x}} + \cos(\alpha) \sin(\phi_k) \hat{\mathbf{y}} + \sin(\alpha) \hat{\mathbf{z}}$ and $\mathbf{k}_4 = -\mathbf{k}_3$.

Now, consider the case where \mathbf{E}_3 is not a plane wave, but an l th order OAM mode whose average wave vector is directed along the positive z axis. As seen above, the OAM beam can be decomposed into an appropriate superposition of plane waves. All that is then necessary is to perform an integration on Eq. (12), similar to the one presented above in Eq. (2), and find that the source term, in this case, can be rewritten as Bessel functions with an overall azimuthal phase dependence.

$$\partial^\mu \partial_\mu \mathbf{E}_4 \approx \omega_0^2 \xi E_1 E_2 E_3^* \mathbf{J}_l(\rho, \phi) e^{i(-\kappa z - \omega_0 t - l\phi)}, \quad (13)$$

where $\beta = k_0 \cos(\alpha)$, $\kappa = k_0 \sin(\alpha)$, and \mathbf{J} is a vector containing the transverse radial dependence of the source.

$$\mathbf{J}_l(\rho, \phi) = \sin(\alpha) J_l(\beta\rho) \hat{\mathbf{z}} + i \cos(\alpha) \frac{J_{l+1}(\beta\rho) - J_{l-1}(\beta\rho)}{2} \hat{\rho} - \frac{l \cos(\alpha) J_l(\beta\rho)}{\beta\rho} \hat{\phi}. \quad (14)$$

Equation (13) can be solved using the standard Green's function method, and the generated field, far from the source, can be written as

$$\mathbf{E}_4 = \frac{(i)^l}{4\pi r c^2} \omega_0^2 \xi E_1 E_2 E_3^* \Lambda_l(\theta) e^{i(k_0 r - \omega_0 t - l\phi)}, \quad (15)$$

where

$$\Lambda_l(\theta) = 2\pi \left[\sin(\alpha) A_l \hat{\mathbf{z}} - \cos(\alpha) \frac{A_{l+1} + A_{l-1}}{2} \hat{\rho} - i \cos(\alpha) \frac{A_{l+1} - A_{l-1}}{2} \hat{\phi} \right], \quad (16)$$

$$A_l = \iint_{V'} e^{-i[\kappa + k_0 \cos(\theta)]} J_{-l}[k_0 \sin(\alpha) \rho'] J_l(\beta\rho') \rho' d\rho' dz', \quad (17)$$

and $r \in \mathbb{R}^+$ is the spherical radial distance from the origin of the finite interaction volume V' whose extent will depend on the size of the focal spots of the three beams being used in the experimental setup. The interaction volume is artificially limited in this calculation because the beams used in the analytical derivation have infinite extent and are nonintegrable over all of space, while physical beams will always have an integrable intensity envelope. The direction of propagation of this generated wave can be seen in the angular dependence of $\Lambda_l(\theta)$ in Fig. 1. From it, we can conclude that the generated wave propagates along the same axis but in the opposite direction as the initial OAM mode \mathbf{E}_3 , which is intuitive as \mathbf{E}_1 and \mathbf{E}_2 are antiparallel, and linear momentum is conserved. It can also be clearly seen in Eq. (15) that the generated field has the opposite azimuthal phase dependence of \mathbf{E}_3 . This means that the OAM of the generated photons will be opposite in sign, which is to be expected as a consequence of conservation of angular momentum since the two other initial waves \mathbf{E}_1 and \mathbf{E}_2 were plane waves. Then we can use Eq. (15) to calculate the generated intensity $I_4 = (1/2) c \epsilon_0 |E_4|^2$ which can be

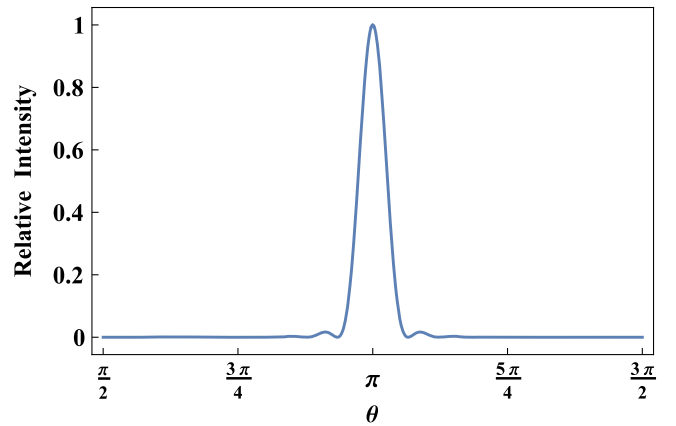


FIG. 1. Plot of the angular dependence of the field of the generated photons $|E_4|^2$ to show the direction of propagation of the generated wave. θ is the polar angle defined, as it usually is in the spherical coordinate system, from the z axis.

integrated over the surface of the interaction volume to calculate the number of generated photons for specific initial laser parameters.

Equation (15) shows that, for a specific set of three-beam geometries, if one of the lasers is carrying some OAM (l), then the photons generated due to photon-photon scattering will carry the opposite value $l_4 = -l$ as can be seen from the azimuthal dependence in the phase of the generated field. We propose to use this additional signature to design a novel high-power laser experiment to verify this hitherto undetected phenomenon. In order to make the generated photons even easier to distinguish, the geometry will be modified slightly from the one considered previously. Instead, consider three initial waves in the configuration outlined in Fig. 2, where $[\mathbf{k}_1 = -2(\omega_0/c)(1/2\hat{\mathbf{z}} + \sqrt{3}/2\hat{\mathbf{x}}), \hat{\mathbf{n}}_1 = \hat{\mathbf{y}}]$ and $[\mathbf{k}_2 = -2(\omega_0/c)(1/2\hat{\mathbf{z}} - \sqrt{3}/2\hat{\mathbf{x}}), \hat{\mathbf{n}}_2 = \hat{\mathbf{y}}]$ are plane waves, and \mathbf{E}_3 is an OAM beam with $l_3 = 1$ and $\omega_3 = \omega_0$ that is propagating along the positive z axis. These kinds of modes can be efficiently generated in the laboratory using mode-conversion methods such as so-called spiral phase mirrors which have efficiently generated OAM-carrying high power lasers [22]. According to Eqs. (11) and (15), we should then expect to detect photons generated at $\omega_4 = \omega_1 + \omega_2 - \omega_3 = 3\omega_0$ with $l_4 = -1$ propagating along the negative z direction. These generated photons are then distinct, from any of the initial radiation in the interaction, in frequency, direction of travel, and OAM state. The expected number of photons generated by photon-photon scattering N_γ can be calculated from Eq. (15) using

$$N_\gamma = \frac{\epsilon_0 c \tau}{2\hbar\omega_4} \int_0^\pi \int_0^{2\pi} |E_4(r, \theta, \phi)|^2 r^2 \sin(\theta) d\theta d\phi, \quad (18)$$

where τ is the duration of the interaction. In the case of a high-power laser of 10 PW at a wavelength of 800 nm, where the laser pulse duration is $\tau = 30$ fs, the beam must be split into three, where two of the component parts are frequency doubled. Considering a second harmonic conversion

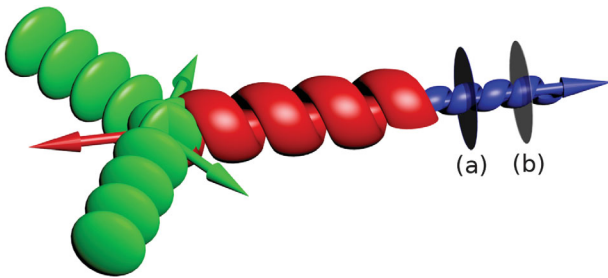


FIG. 2. A sketch of the proposed geometry for the experiment showing the three main initial beams. The $2\omega_0$ (green) beams have a flat phase front whereas the ω_0 (red) beam has a helical front arising from the nonzero OAM. The figure illustrates the generated $3\omega_0$ (blue) spiral photons. (a) and (b) are the frequency and OAM filters, respectively, which will be used to remove background noise.

efficiency of 30% and a spot size of $5 \mu\text{m}$, Eq. (18) predicts that N_γ is expected to be on the order of 100 photons per shot. It should be noted that, since unphysical light modes were used for this derivation, it can only provide an initial estimate of the number of generated photons through photon-photon scattering. However, this is not a major concern as any additional realistic envelope (such as a Gaussian envelope) will vary slowly compared to the oscillations of the field and, as such, will have negligible contributions to the photon-photon scattering interaction. Figure 3 shows the scaling of N_γ with respect to the power of the initial laser, while keeping all other parameters the same as the above example. Comparing this scaling to the one in the case with no OAM [5], it is clear that the introduction of OAM does not change the coupling strength of the photon-photon interaction and the predicted number of photons generated from it is of the same order when laser parameters are matched.

Although the number of photons may seem small, especially compared to the other three high-power beams [e.g., the OAM-carrying beam contains $O(10^{20})$ photons], its multiple different signatures will allow for efficient filtering of any other background radiation. There have been many successful experiments where even single photons have been filtered by their OAM state and detected using highly efficient single-photon detectors [12,21]. Along with OAM filtering, frequency filtering with ultra-narrow-band bandpass filters would block any photons whose frequency is sufficiently different from what is expected from the previously defined three-beam interaction. The single-photon detectors can also be gated to only be sensitive to scattered photons that are generated during the interaction time in order to further reduce the noise. Furthermore, performing this experiment on a high-power and high-repetition rate laser facility, such as the ELI facility [27,28] or the Apollon facility [29], would allow for gathering the statistics essential for verification of the scattering event. The scattering signal would also be boosted

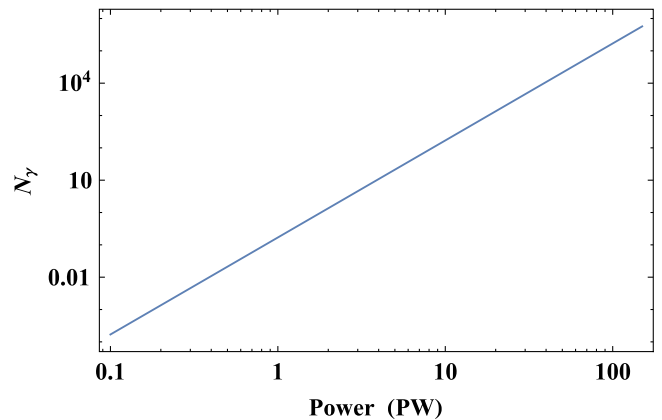


FIG. 3. Plot showing the scaling of the estimated number of generated photons as a function of initial laser power while fixing all other laser parameters (focal spot and pulse duration).

by orders of magnitude by performing the experiment on the upcoming 100 PW Station of Extreme Light (SEL) laser facility as may be seen from the scaling in Fig. 3.

Of course, it is practically impossible to achieve a perfect vacuum even in a laboratory setting. Even within a vacuum chamber, there are still some particles that can interact with the lasers and generate some noise. The main interaction contributing to this concern is Compton scattering. However, as shown in [5], the number of Compton-scattered photons that would possibly be generated in the appropriate frequency band is much smaller than the photon-photon scattering signal we expect. Also, as proven in [30], the OAM state of these Compton-scattered photons would either be 0 or the opposite of the state of interest. Thus, using a projective OAM filtering technique [31], the already small amount of noise can be reduced by 25 dB compared to the case without the OAM signature while the signal remains as strong, thus, making detection of the signal of interest feasible.

In this Letter, we have investigated the effect of orbital angular momentum on elastic photon-photon scattering. Using effective field theory, we have derived an expression for the expected generated field. We have shown that the OAM coupling will provide an additional useful signature for the interaction and will allow for the use of quantum optics techniques to discern them from any background radiation. We have also proposed an experimental setup, which we plan to perform at the SEL laser facility, that would allow for the detection of this effect using high-power lasers. The experimental verification of the polarization of the vacuum will open a new era in strong field, low energy quantum electrodynamics for fundamental physics investigations.

We thank all of the staff of the Central Laser Facility, Rutherford Appleton Laboratory and, in particular, Prof. David Neely for stimulating discussions. This work was supported by UKRI-STFC and UKRI-EPSC under Grants No. ST/P002048/1 and No. EP/N509711/1. R. A. acknowledges support from the St Anne's Graduate Development Scholarship scheme.

*ramy.aboushelbaya@physics.ox.ac.uk

†Also at John Adams Institute for Accelerator Science, University of Oxford, Denys Wilkinson Building, Keble Road, Oxford OX1 3RH, United Kingdom.

- [1] G. Brodin, M. Marklund, and L. Stenflo, *Phys. Rev. Lett.* **87**, 171801 (2001).
- [2] A. E. Kaplan and Y. J. Ding, *Phys. Rev. A* **62**, 043805 (2000).
- [3] V. B. Berestetskii, L. D. Landau, E. M. Lifshitz, and L. P. Pitaevskii, *Quantum Electrodynamics* (Butterworth-Heinemann, Oxford, 1982).
- [4] B. Shen, M. Y. Yu, and X. Wang, *Phys. Plasmas* **10**, 4570 (2003).
- [5] E. Lundstrom, G. Brodin, J. Lundin, M. Marklund, R. Bingham, J. Collier, J. T. Mendonca, and P. Norreys, *Phys. Rev. Lett.* **96**, 083602 (2006).
- [6] B. King, H. Hu, and B. Shen, *Phys. Rev. A* **98**, 023817 (2018).
- [7] *Twisted Photons: Applications of Light with Orbital Angular Momentum*, edited by J. P. Torres and L. Torner, 1st ed. (Wiley-VCH, Weinheim, Germany, 2011).
- [8] L. Allen, M. W. Beijersbergen, R. J. C. Spreeuw, and J. P. Woerdman, *Phys. Rev. A* **45**, 8185 (1992).
- [9] T. Lei, S. Gao, Z. Li, Y. Yuan, Y. Li, M. Zhang, G. N. Liu, X. Xu, J. Tian, and X. Yuan, *IEEE Photonics J.* **9**, 1 (2017).
- [10] S. R. Ghaleh, S. Ahmadi-Kandjani, R. Kheradmand, and B. Olyaeefar, *Appl. Opt.* **57**, 9609 (2018).
- [11] R. H. Hadfield, *Nat. Photonics* **3**, 696 (2009).
- [12] J. Leach, M. J. Padgett, S. M. Barnett, S. Franke-Arnold, and J. Courtial, *Phys. Rev. Lett.* **88**, 257901 (2002).
- [13] W. Heisenberg and H. Euler, *Z. Phys.* **98**, 714 (1936).
- [14] M. Abramowitz, *Handbook of Mathematical Functions, With Formulas, Graphs, and Mathematical Tables* (Dover Publications, Inc., New York, 1974).
- [15] D. McGloin and K. Dholakia, *Contemp. Phys.* **46**, 15 (2005).
- [16] J. C. Maxwell, *Phil. Trans. R. Soc. London* **155**, 459 (1865).
- [17] See Supplemental Material at <http://link.aps.org/supplemental/10.1103/PhysRevLett.123.113604> for a more detailed derivation of the nonlinear wave equation and a more in-depth explanation of the elements contributing to the increase of the signal-to-noise ratio, which includes Refs. [18–26].
- [18] G. Campbell, B. Hage, B. Buchler, and P. K. Lam, *Appl. Opt.* **51**, 873 (2012).
- [19] D. Ganic, X. Gan, M. Gu, M. Hain, S. Somalingam, S. Stankovic, and T. Tschudi, *Opt. Lett.* **27**, 1351 (2002).
- [20] A. Longman and R. Fedosejevs, *Opt. Express* **25**, 17382 (2017).
- [21] A. Nicolas, L. Veissier, L. Giner, E. Giacobino, D. Maxein, and J. Laurat, *Nat. Photonics* **8**, 234 (2014).
- [22] A. Longman, C. Salgado, G. Zeraouli, J. I. Apinani, J. A. Perez-Hernandez, M. De Marco, C. He, G. Gatti, L. Volpe, W. T. Hill, and R. Fedosejevs, 60th Annual Meeting of the APS Division of Plasma Physics **63**, 11 (2018), <http://meetings.aps.org/link/BAPS.2018.DPP.JO8.2>.
- [23] A. Longman and R. Fedosejevs (private communication).
- [24] A. Nicolas, L. Veissier, E. Giacobino, D. Maxein, and J. Laurat, *New J. Phys.* **17**, 033037 (2015).
- [25] V. G. Shvedov, C. Hnatovsky, W. Krolikowski, and A. V. Rode, *Opt. Lett.* **35**, 2660 (2010).
- [26] A. Hervy, L. Gallais, G. Cheriaux, and D. Mouricaud, *Opt. Eng.* **56**, 011001 (2016).
- [27] J.-P. Chambaret *et al.*, *Proc. SPIE* **7721**, 77211D (2010).
- [28] G. Mourou and T. Tajima, *Opt. Photonics News* **22**, 47 (2011).
- [29] D. N. Papadopoulos, J. P. Zou, C. Le Blanc, G. Chriaux, P. Georges, F. Druon, G. Mennerat, P. Ramirez, L. Martin, A. Frneaux, A. Beluze, N. Lebas, P. Monot, F. Mathieu, and P. Audebert, *High Power Laser Sci. Eng.* **4**, E34 (2016).
- [30] U. D. Jentschura and V. G. Serbo, *Phys. Rev. Lett.* **106**, 013001 (2011).
- [31] A. Nicolas, L. Veissier, E. Giacobino, D. Maxein, and J. Laurat, *New J. Phys.* **17**, 033037 (2015).